ORIGINAL ARTICLE

Accurate Quantification of Choline-to-Creatine Ratio as a Biomarker to Distinguish Osteosarcoma Patients from Normal Subjects Employing Proton Magnetic Resonance Spectroscopy Imaging at 3 Tesla

Shaghayegh Karimi Alavijeh [1,2], Fakhereh Pashaei [3], Mahrooz Malek [4], Hamidreza Saligheh Rad [1,2*] ID

[1] Department of Medical Physics and Biomedical Engineering, School of Medicine, Tehran University of Medical Sciences, Tehran, Iran

[2] Quantitative MR Imaging and Spectroscopy Group, Research Center for Cellular and Molecular Imaging, Tehran University of Medical Sciences, Tehran, Iran

[3] Radiation Sciences Research Center, Aja University of Medical Sciences, Tehran, Iran

[4] Advanced Diagnostic and Interventional Radiology Research Center, Tehran University of Medical Sciences, Tehran, Iran

*Corresponding Author: Hamidreza Saligheh Rad
Email: h-salighehrad@tums.ac.ir

Abstract

Purpose: This study focused on accurate quantification of a maximum of Choline-to-Creatine ratio (Max (Cho/Cr)) in 10 Osteosarcoma patients, in comparison with 5 healthy volunteers as our control group using proton Magnetic Resonance Spectroscopy Imaging (1H-MRSI).

Materials and Methods: Max (Cho/Cr) were obtained in 10 patients with Osteosarcoma over their corresponding ratio maps containing diseased tissue, to be compared with Cho/Cr in 5 healthy volunteers at 3T, employing MRSI (Performed Employing Pointed-resolved Spectroscopy (PRESS), TR/TE: 2500s /135 ms) with water-suppression. An extra unsuppressed water Single-Voxel Spectroscopy (SVS) was acquired to provide phase information for further Eddy Current Correction (ECC). Multi-stage preprocessing was applied. Subtract QUEST MRSI as a time-domain technique was employed to accurately quantify the metabolites' ratios and to estimate the baseline.

Results: An optimal database for Subtract QUEST was achieved based on multiple trials evaluated by acceptable peak-fitting and Cramer-Rao-Bound (CRB). Lipids at frequencies of 0.94 and 1.33ppm were combined to increase the accuracy of the Lipid estimation.

Conclusion: Estimation of Max (Cho/Cr) evaluated over Cho/Cr spatial maps to distinguish Osteosarcoma patients from normal subjects suggested that the proposed quantification method leads to high power and linear classifier with a high degree of reproducibility, considering 1H-MRSI at 3T machine as a high efficacy diagnostic tool for musculoskeletal radiology.

Keywords: Magnetic Resonance Spectroscopy; Magnetic Resonance Spectroscopy Imaging; Metabolite; Osteosarcoma; Subtract Quantum Estimation.

1. Introduction

1H-MRSI is a none-invasive quantitative diagnostic method that is able to analyze biochemical macromolecules, pathological changes and quantitatively determine metabolites to monitor response to therapy of tumors [1, 2], and in different parts of the body [3, 4] (such as the brain [5-7], breast [8,9], prostate and kidney [10,11], and liver [12]). 1H-MRSI along with accurate quantification of metabolites with spatial localization has recently attracted lots of attention in Musculoskeletal (MSK) applications in general [13-19], and in Osteosarcoma in particular [14, 15, 17].

Osteosarcoma is a primary malignant tumor of bone that often occurs inside or on the surface of the long bone [20]. Early diagnosis of this disease and its response to therapy is a significant factor for appropriate treatment planning. Each imaging modality such as radiography, Magnetic Resonance Imaging (MRI), Computed Tomography (CT scan) or bone scintigraphy has deficiencies to diagnose this disease. Biopsy, however, is the most specific method to specify the tissue type which shall be performed after imaging as the final step, but is known to be invasive and may have adverse effects if applied with any small mistake [15,20,21]. Employing 1H-MRSI, we can detect important molecular information from the tissue under investigation and its metabolites. Choline peak and also Choline-containing compounds (phosphocholine and glycerolphosphocholine), visible at 3.2 ppm of the magnetic resonance (MR) spectrum and constituents of the phospholipid metabolism of cell membranes reflecting cellular proliferation, has been discussed as the biomarker of malignancy in MSK tumors [14-18,13,19]. Such spectroscopy mechanism not only identifies accurate chemical composition of the organ under study, but also provides the clinical expert with spatial information of the heterogeneity, the borders and the extension of the tumorous region [3]. One key factor to successfully employ the MRSI method for disease diagnosis purposes depends on how metabolites are estimated after the acquisition, called the quantification method, which is performed either in the frequency domain or in the time domain. In this work, we optimally employed Subtract-QUEST as an accurate time-domain quantification algorithm for precise estimation of the Max(Cho/Cr), evaluated over spatial grids of Cho/Cr maps containing tissues with Osteosarcoma [22]. This nonlinear least-squares algorithm fits a time-domain model function, created with quantum mechanical simulation techniques employing NMR-SCOPE, to low- Signal to Noise Ratio (SNR) in-vivo signal [23]. The quantification procedure was optimally designed in two steps: 1) pre-processing, including ECC, SNR enhancement, phase correction, and residual water removal, and 2) ratio quantification, including optimal design of the metabolites' database achieved via multiple trials evaluated by approving criteria, as well as an optimal selection of the algorithm parameters. Results achieved by 1H-MRSI showed significant differences between estimated metabolite ratios in tumorous areas against normal subjects. These differences were then depicted by their color maps, precisely overlaid on the anatomical images.

2. Materials and Methods

2.1. Data Acquisition and Quantification

2.1.1. Subjects

10 patients (9 men; mean age, 30 years old; age range, 15-35 years and 1 woman, age: 42) with 10 Osteosarcoma bone tumors were included in our clinical study. All lesions were previously diagnosed by a skilled MSK radiologist employing CT scan and conventional MRI, and were histologically analyzed and confirmed by an expert pathologist. Informed consent was obtained from each patient after explaining the MR imaging and spectroscopy techniques before the examination. Grading of these tumors was not considered in our study. The control group included 5 healthy volunteers (5 women; mean age, 27.8 years old, age range, 25-34 years). MRI and MRS examinations were applied on the vastus medialis and vastus intermedius muscles of the distal part of the right femur in our healthy volunteers.

2.1.2. MR Imaging and Spectroscopy

All examinations were performed on a 3T Siemens Magnetom TIM Trio scanner (Siemens, Erlangen, Germany). All 10 patients were examined in the supine position. Combinations of spine and body matrix coils were used to optimally collect the MRS signal. The imaging session started with anatomical imaging to show the MSK lesions in specific Field-Of-View (FOV) as follows: axial, sagittal, and coronal images were obtained using a proton density-weighted spin-echo sequence, TE/TR = 32/2900 ms, flip angle = 90°, matrix size = 256×256 and FOV = 140×140cm^2 covering the tumorous region. An MSK radiologist

determined the position of the MRSI grid based on the anatomical MRI image. Enhancing contrast agent was not used before MRS examination to avoid metabolic changes caused by injected contrast materials [15]. Next, 1H-MRSI was PRESS pulse sequence [24], TE/TR = 135/2500 ms, flip angle = 90°, sampling interval = 0.833 ms, number of data points = 1024 and bandwidth = 1200 Hz. Outer-Volume Suppression (OVS) was applied to attenuate the unwanted signals from outside the grid. Water suppression using Chemical Shift Selective Imaging Sequence (CHESS) pulses were performed to evaluate Cho/Cr more accurately [25]. No lipid suppression was applied. Receiver gain adjustments and automated optimization of frequency, and gradient tuning were performed. To compensate for magnetic field inhomogeneity, automated and manual shimming was performed. FOV size in the MRSI examination was specifically adjusted for each patient to provide enough spatial information of heterogeneity, borders, and extension of the tumorous region.

In the current study, an additional SVS without water suppression was acquired to provide the phase information, employing PRESS technique with TE/TR =135/2500 ms, flip angle=90°, sampling interval= 0.833 ms, number of data points =1024, and bandwidth =1200 Hz. The duration of each examination was about 15 minutes. The same imaging protocols for both anatomical and functional MR imaging were applied on the healthy volunteers. A knee coil with 8 channels was used to acquire MRS signal from the distal part of the femur of volunteers and the size of Volume Of Interest (VOI) was the same as the tumor groups. All received signals were saved in a channel-by-channel fashion to be able to correct for phase distortions caused by each channel element.

2.1.3. Pre-Processing

The preprocessing of the Free Induction Decay (FID) signal before the main quantification is crucial for the better interpretation of 1H-MRS data. This step was performed similarly in both patients and normal groups.

Multi-stage preprocessing was individually applied on the signal acquired from each coil element to compensate for some phase artifacts and to optimize spectral analysis, as follows: 1) ECC [24]; rapid switching of the magnetic field gradients during data acquisition causes eddy currents in metal structures such as main magnet coils and Radio Frequency (RF) coils, resulting in signal loss and phase variations. To correct eddy currents, an unsuppressed water signal (in an SVS) was acquired as an internal reference.

The phase of the water signal was determined in each time point and then it was subtracted from the phase of the acquired signal; 2) SNR enhancement [24], the recorded FID signal during MRS acquisition consists of signal and noise. The thermal motion of the electrons in coils is the most important source of noise in the MRS signal. SNR improvement was performed by the multiplication of the received signal by a negative exponential, amplifying the beginning of the signal and suppressing its end; 3) Phase correction; due to some instrumental imperfections, MRS spectra are not zero-phased, i.e. there is a distorted phase shift or phase error in the spectrum, leading to distortion in spectrum shape and resulting in inappropriate spatial resolution and metabolite estimation. Therefore, phase correction was performed in two steps after using Fourier transformation as bellows: a) zero-order phase correction, including the multiplication of the same degree of phase correction by the entire spectrum, and b) first-order phase correction that was performed by changing the rate of change of phase employing frequency and 4) Water removal [3, 24], since the residual water remains even after water suppression during data acquisition, it was necessary to decrease the high peak of water that overlaps the other MSK metabolite's peaks such as Cho, Cr, and Lipids (in 0.94ppm and 1.33ppm), and employing maximum-phase Finite Impulse Response (MP-FIR) filter [25].

2.1.4. Quantification

Subtract-QUEST-MRSI, a nonlinear least-square algorithm, was employed to accurately quantify the metabolites ratios and to estimate the baseline and the white Gaussian noise. This time-domain quantification algorithm fits a time-domain model function (a combination of metabolites' signals, either generated by simulation or by measurement) to a low SNR signal in-vivo. In this work, we generated the dictionary of metabolites in NMR-SCOPE of jMRUI software using the spin Hamiltonian parameters that enable to handle various experimental protocols (such as PRESS and STimulated Echo Acquisition Mode (STEAM)) at the appropriate magnetic fields.

An optimal database for metabolites is needed for the Subtract-QUEST-MRSI algorithm to optimally estimate the concentration of metabolites of interest, which was achieved here with trials and errors, i.e., by adding different metabolites to and removing from the database where lipids at frequencies of 0.94 and 1.33 ppm were combined to minimize Lipid quantification error. The optimal database was then evaluated by approving statistical criteria,

including minimum reconstruction artifacts, acceptable peak fitting and eligible range of CRB [24].

As far as the metabolites ratio quantification goes, Max (Cho/Cr) was evaluated over the spatial region where Osteosarcoma tissues were found by our MSK radiologist. This number was then compared with Cho/Cr of the control group estimated exactly in voxels located in vastus medialis and vastus intermedius muscles where there was no lipid contamination or partial voluming from neighboring voxels. This ratio was reported as a mean value ± Standard Deviation (SD). Mean values between lesions and healthy volunteers were compared using an independent two-tailed, unequal variance t-test. Intraclass Correlation Coefficient (ICC) was calculated for the control group to assess the reproducibility of the examination. Statistical significance was set at $p < 0.01$.

3. Results

In Figure 1 we have shown the best database optimized for MRS quantification of Osteosarcoma employing subtract-QUEST-MRSI, resulting in Alanine (Ala), Cr, Lactate, Lipids (at both 0.94 and 1.33ppm), and water to calculate Max (Cho/Cr). Here Cho is composed of Cho (at 3.2ppm), phosphocholine (at 3.2 and 3.63ppm), and glycerolphosphocholine (at 3.21 ppm) [26].
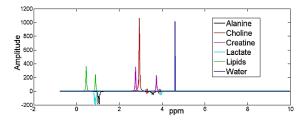

Figure 1. Optimized database to calculate the Max(Cho/Cr) in osteosarcoma and from the water-suppressed MRSI was obtained after many trials and errors, resulting in the combination of Ala (1.47 ppm), Cho (3.21 ppm), Cr (3.02 and 3.91 ppm), Lac (1.31 ppm that is reversed versus Lipid at TE=135ms), Lipids (at frequencies of 0.94 and 1.33ppm), and water (4.7ppm). The Cho signal includes the Cho (at 3.2ppm), phosphocholine (at 3.2 and 3.63ppm) and glycerolphosphocholine (at 3.21ppm) signals

As stated earlier, and in order to have a more accurate estimation for the Lipid, two peaks of lipid at 0.94 ppm and 1.33 ppm were combined to generate one single lipid metabolite [26]. Figure 2 shows the lipid signals and their results before and after combination.
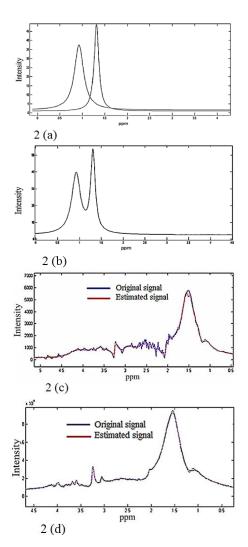

2 (a)

2 (b)

2 (c)

2 (d)

Figure 2. (a) Lipid peaks including lipid at 0.94 and 1.33 ppm at TE=135 msce (before modification), (b) Combination of two Lipids at frequencies of 0.94 and 1.33 ppm (after modification), (c) Peak-fitting before the combination of the two Lipids, and (d) Peak-fitting after combination of two the Lipids. The value of noise is lower in the figure that shows the peak fitting after combination of the two Lipids at two different frequencies.

In order to correct phase distortions generated by each individual channel element of the coil, signals received from each channel element were separately saved in different files and a channel-by-channel fashion, followed by individual application of pre-processing steps on each channel element signal.

Finally, pre-processed signals from different channel elements were combined to generate the high SNR signa to be quantified (as shown in Figure 3).

For better visualization of the quantification results, an appropriate color map was generated to show the changes of the quantified Cho/Cr in the FOV under investigation, and as follows: Red-colored voxels indicate the hot regions where the metabolite concentration ratios are high and

vice versa for the blue-colored voxels. The generated maps were overlaid on the anatomical images acquired before the functional imaging. Figure 4 shows a coronal image from a 26-year-old man with Osteosarcoma of the right humerus, along with the overlaid map of the Cho/Cr ratio where the red area is placed on high biological activity areas [26].

Table 1 shows the quantification results of Max (Cho/Cr) in the patients, as well as Cho/Cr in the control group and different voxels of the FOV presented in mean ± SD, showing values of 0.46 ± 0.04 and 0.34 ± 0.05 for Max (Cho/Cr) in the patients and Cho/Cr in the control group, respectively. Results verify a statistically significant increase of about 35% (P < 0.0001) in the Cho/Cr from

the normal subjects to Max (Cho/Cr) in patients with tumorous lesions (as depicted in Figure 5).

Figure 6 shows a scatter plot of the test-retest data as well as ICC result, indicating the reproducibility with R-square of 0.80% with ICC of 0.80%.

The reliability of the quantification results was estimated employing CRB; CRB calculates quantification errors that are caused by insufficient modeling of the background signal and noise, coded with green color as the accuracy with a probability of higher than 50%, white color as the accuracy with a probability of higher than 20% and lower than 50%, and red color as the accuracy with a probability of lower than 20%.
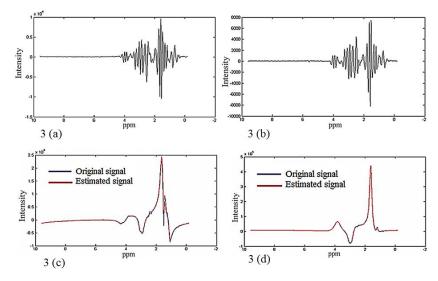

Figure 1. Noise and the peak fitting results in two different methods used for data acquisition: (a) All received signals saved in a channel-by-channel fashion for individual pre-processing steps, (b) Single acquired from the scanner, (c) Peak fitting results achieved by the first method, and (d) Peak fitting results achieved by the second method
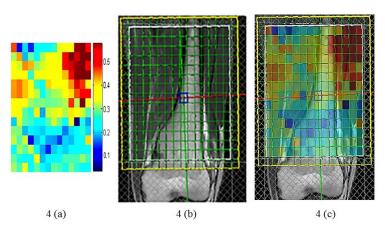

Figure 4. Quantification results on a 26-year-old male with osteosarcoma in his right femur: (a) Metabolite map obtained after applying subtract-QUEST-MRSI algorithm according to the value of the Cho/Cr in different voxels to pictorially show the differences for better visualization. The scale to the right shows the values for the colors and metabolite ratios varying from 0.08 to 0.6 in different voxels. In the voxels with higher Max (Cho/Cr), the color is red, and for voxels with lower Max (Cho/Cr) the color is blue. (b) Anatomical image of the tissue under investigation, and (c) Distribution of the Max (Cho/Cr) overlaid on the associated the anatomical MRI image

Table 1. represents results of Max (Cho/Cr) for 10 patients and Cho/Cr in 5 volunteers, with average values of 0.46 ± 0.04 and 0.34 ± 0.05, respectively. Measurements are performed in a number of voxels that are specified in the table

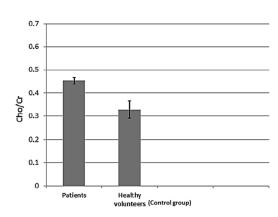| Patients	Number of Voxels	Max (Cho/Cr) (Mean, SD)	Volunteers	Number of Voxels	Cho/Cr (Mean, SD)
Patient 1	18	0.43±0.01	Volunteer 1 Series 1	7	0.31±0.05
Patient 2	30	0.44±0.02	Volunteer 1 Series 2	7	0.31±0.04
Patient 3	22	0.47±0.05	Volunteer 2 Series 1	5	0.32±0.03
Patient 4	24	0.42±0.04	Volunteer 2 Series 2	5	0.33±0.06
Patient 5	14	0.55±0.11	Volunteer 3 Series 1	8	0.33±0.04
Patient 6	54	0.49±0.05	Volunteer 3 Series 2	8	0.33±0.08
Patient 7	12	0.45±0.03	Volunteer 4 Series 1	7	0.35±0.03
Patient 8	15	0.43±0.04	Volunteer 4 Series 2	7	0.34±0.06
Patient 9	31	0.45±0.02	Volunteer 5 Series 1	4	0.35±0.01
Patient 10	27	0.45±0.02	Volunteer 5 Series 2	4	0.36±0.04

Figure 5. Quantification results of the Max (Cho/Cr) in two groups of 10 patients and 5 normals show a statistically significant difference of 35 % ($p < 0.0001$) between the patient and the control groups

6 (a)

6 (b)

Figure 6. In our control group, the MRS examination was performed twice for each person to compute the reproducibility in test-retest format: (a) R2 = 0.8, and (b) ICC = 0.8

4. Discussion

To our knowledge, investigation of Max (Cho/Cr) ratio employing 1H-MRSI at 3T in MSK tumors in general and for Osteosarcoma in particular, has not been previously reported. MRSI, as a none-invasive diagnostic tool, can provide information about metabolite distribution in the area under investigation. The SNR and the level of Cho, which includes the signal of three metabolites as Cho, phosphocholine and glycerolphosphocholine, have been considered as a biomarker of malignancy in MSK tumors [13, 14, 19, 17, 16]. In benign MSK lesions, the Cho peak and the Cho/Cr ratio are lower in comparison with malignancies [17]. In this study, the
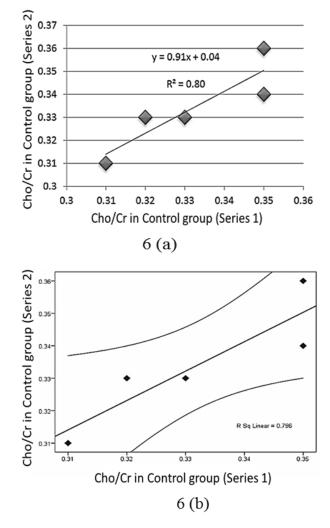
Max (Cho/Cr) evaluated over the spatial grid with Osteosarcoma tissues considering as a marker for making a differentiation between patients with Osteosarcoma and the control normal group was 1.36 ± 0.8. According to Qi zi-hue [17], the value of Cho/Cr ratio in musculoskeletal tumors starts from 1.45 ± 1.03. Here we found that these numerical reports depend on the method of quantification and baseline estimation. The better baseline estimation performs, the more accurate metabolite estimation occurs. Ratiney *et al.* [22] stated that the Subtract_QUEST_MRSI quantification algorithm, which is also employed in this study, is a powerful method to estimate the signal caused by lipids and macromolecules which is known as baseline.

Some limitations in our study are as follows: 1) the grade of Osteosarcoma was not considered in this work. It is shown that statistically important difference in Cho concentration between grade 1 and other grades of malignant bone and soft tissue tumors [18]. In this light, considering a larger group of samples, including several kinds of diseases is useful to evaluate the grade of this disease; 2) In this study, Osteosarcoma in all parts of the musculoskeletal system such as femur, tibia, humerus, and clavicle of males and females were considered, which may affect the obtained results in that the ratio changes from tissue to tissue, as shown by Fayad *et al.* [19] for Cho concentration in right and left muscle groups, as well as in males and females; 3) In order to accurately estimate the absolute values of Cho and Cr in different locations, an accurate map of B1 received field is required in the area under investigation, which is an extremely difficult task to perform when using body matrix coils [9].

5. Conclusion

In conclusion, employing proton MRSI as a supplementary diagnostic tool along with the subtract-QUEST-MRSI quantification algorithm as an accurate time-domain quantification method, we managed to observe meaningful changes in Max (Cho/Cr) to distinguish Osteosarcoma patients from normal subjects. The best quantification database was optimized for the quantification of MRSI data acquired in Osteosarcoma. Appropriate color maps were generated to depict Cho/Cr changes in the tissue under investigation. The best pre-processing stages were optimized to be applied on the MRS signal and in a channel-by-channel fashion. A threshold was defined for Max (Cho/Cr) as a biomarker to distinguish Osteosarcoma.

As future work, we suggest making a comparison between the values of the diagnostic biomarker before and after chemotherapy to achieve the optimal treatment and surgical planning.

Acknowledgements

References

1- Ċ. Carlsson, "Susceptibility effects in MRI and 1H MRS. The spurious echo artifact and susceptibility measurements." *Department of Physics; Institutionen för fysik*, 2009.

2- J. B. Lambert and E. P. Mazzola, "Nuclear Magnetic Resonance Spectroscopy An Introduction to Principles, Applications and Experimental Methods (paper)," *Recherche*, vol. 67, p. 02, 2003.

3- P. K. Mandal, "< i> In vivo</i> proton magnetic resonance spectroscopic signal processing for the absolute quantitation of brain metabolites," *European journal of radiology*, vol. 81, no. 4, pp. e653-e664, 2012.

4- I. C. Smith and L. C. Stewart, "Magnetic resonance spectroscopy in medicine: clinical impact," *Progress in Nuclear Magnetic Resonance Spectroscopy*, vol. 40, no. 1, pp. 1-34, 2002.

5- R. E. Jung, C. Gasparovic, R. S. Chavez, A. Caprihan, R. Barrow, and R. A. Yeo, "Imaging intelligence with proton magnetic resonance spectroscopy," *Intelligence*, vol. 37, no. 2, pp. 192-198, 2009.

6- A. K. Singh, A.-M. Wang, and W. Sanders, "Magnetic resonance spectroscopy of the brain," *APPLIED RADIOLOGY*, vol. 31, no. 12; SUPP/2, pp. 58-65, 2002.

7- A. Di Costanzo *et al.*, "Proton MR spectroscopy of the brain at 3 T: an update," *European radiology*, vol. 17, no. 7, pp. 1651-1662, 2007.

8- P. Stanwell and C. Mountford, "In Vivo Proton MR Spectroscopy of the Breast1," *Radiographics*, vol. 27, no. suppl 1, pp. S253-S266, 2007.

9- P. J. Bolan, M. T. Nelson, D. Yee, and M. Garwood, "Imaging in breast cancer: magnetic resonance spectroscopy," *Breast Cancer Res*, vol. 7, no. 4, pp. 149-152, 2005.

10- F. G. Claus, H. Hricak, and R. R. Hattery, "Pretreatment Evaluation of Prostate Cancer: Role of MR Imaging and 1H MR Spectroscopy1," *Radiographics*, vol. 24, no. suppl 1, pp. S167-S180, 2004.

11- R. Kumar, M. Kumar, N. Jagannathan, N. P. Gupta, and A. K. Hemal, "Proton magnetic resonance spectroscopy with a body coil in the diagnosis of carcinoma prostate," *Urological research*, vol. 32, no. 1, pp. 36-40, 2004.

12- A. Qayyum, "MR spectroscopy of the liver: principles and clinical applications," *Radiographics*, vol. 29, no. 6, pp. 1653-1664, 2009.

13- S. Doganay, T. Altinok, A. Alkan, B. Kahraman, and H. M. Karakas, "The role of MRS in the differentiation of benign and malignant soft tissue and bone tumors," *European journal of radiology*, vol. 79, no. 2, pp. e33-e37, 2011.

14- C.-K. Wang, C.-W. Li, T.-J. Hsieh, S.-H. Chien, G.-C. Liu, and K.-B. Tsai, "Characterization of Bone and Soft-Tissue Tumors with in Vivo 1H MR Spectroscopy: Initial Results1," *Radiology*, vol. 232, no. 2, pp. 599-605, 2004.

15- L. M. Fayad, D. A. Bluemke, E. F. McCarthy, K. L. Weber, P. B. Barker, and M. A. Jacobs, "Musculoskeletal tumors: use of proton MR spectroscopic imaging for characterization," *Journal of Magnetic Resonance Imaging*, vol. 23, no. 1, pp. 23-28, 2006.

16- L. M. Fayad *et al.*, "Characterization of musculoskeletal lesions on 3-T proton MR spectroscopy," *American Journal of Roentgenology*, vol. 188, no. 6, pp. 1513-1520, 2007.

17- Z.-h. Qi, C.-f. Li, Z.-f. Li, K. Zhang, Q. Wang, and D.-x. Yu, "Preliminary study of 3T 1H MR spectroscopy in bone and soft tissue tumors," *Chinese Medical Journal (English Edition)*, vol. 122, no. 1, p. 39, 2009.

18- C. W. Lee *et al.*, "Proton magnetic resonance spectroscopy of musculoskeletal lesions at 3 T with metabolite quantification," *Clinical imaging*, vol. 34, no. 1, pp. 47-52, 2010.

19- L. M. Fayad *et al.*, "Quantification of Muscle Choline Concentration by Proton MR Spectroscopy at 3 Tesla: Technical Feasibility," *AJR. American journal of roentgenology*, vol. 194, no. 1, p. W73, 2010.

20- D. S. Geller and R. Gorlick, "Osteosarcoma: a review of diagnosis, management, and treatment strategies," *Clinical advances in hematology & oncology: H&O*, vol. 8, no. 10, p. 705, 2010.

21- M. J. Klein and G. P. Siegal, "Osteosarcoma anatomic and histologic variants," *American journal of clinical pathology*, vol. 125, no. 4, pp. 555-581, 2006.

22- H. Ratiney, M. Sdika, Y. Coenradie, S. Cavassila, D. v. Ormondt, and D. Graveron-Demilly, "Time-domain semi-parametric estimation based on a metabolite basis set," *NMR in Biomedicine*, vol. 18, no. 1, pp. 1-13, 2005.

23- D. Graverondemilly, A. Diop, A. Briguet, and B. Fenet, "Product-operator algebra for strongly coupled spin systems," *Journal of Magnetic Resonance*, Series A, vol. 101, no. 3, pp. 233-239, 1993.

24- F. Jiru, "Introduction to post-processing techniques," *European journal of radiology*, vol. 67, no. 2, pp. 202-217, 2008.

25- A. Bizzi, N. De Stefano, R. Gullapalli, and D. D. Lin, "Clinical MR spectroscopy: techniques and applications." *Cambridge University Press*, 2010.

26- Karimi Alavijeh Sh, Madadi A, Oghabian MA, Malek M, Salighe Rad HR "Accurate quantification of Cho/Cr in Osteosarcoma employing clinical 1H-MRSI at 3T; a comparison study with normal tissue." *In: Proceedings of the 30th scientific meeting, European Society for Magnetic Resonance in Medicine and Biology, France*, p, 2013.